ISSN 1063-7826, Semiconductors, 2010, Vol. 44, No. 11, pp. 1486–1491. © Pleiades Publishing, Ltd., 2010.
Original Russian Text © V.B. Shmagin, V.P. Kuznetsov, K.E. Kudryavtsev, S.V. Obolensky, V.A. Kozlov, Z.F. Krasil'nik, 2010, published in Fizika i Tekhnika Poluprovodnikov, 2010, Vol. 44, No. 11, pp. 1533–1538.

WORKSHOP

Electrical and Luminescence Properties of Silicon-Based Tunnel Transit-Time Light-Emitting Diodes $p^+/n^+/n$-Si:Er

V. B. Shmagin[a]^, V. P. Kuznetsov[b], K. E. Kudryavtsev[a], S. V. Obolensky[c], V. A. Kozlov[a], and Z. F. Krasil'nik[a]

[a] *Institute for Physics of Microstructures, Russian Academy of Sciences, Nizhni Novgorod, 603950 Russia*
^e-mail: shm@ipm.sci-nnov.ru
[b] *Physicotechnical Research Institute, Lobachevsky State University, Nizhni Novgorod, 603950 Russia*
[c] *Lobachevsky State University, Nizhni Novgorod, 603950 Russia*

Submitted April 8, 2010; accepted for publication April 20, 2010

Abstract—The electrical and luminescence properties of silicon-based tunnel transit-time light-emitting diodes (LEDs) $p^+/n^+/n$-Si:Er, emitting under reverse bias on the p^+/n^+ junction in the breakdown regime, have been investigated. The room-temperature emission power at the wavelength $\lambda \approx 1.5$ μm (~5 μW), external quantum efficiency (~10^{-5}), and excitation efficiency of erbium ions (~2×10^{-20} cm^2 s) have been determined. At the same excitation efficiency, tunnel transit-time LEDs exhibit higher emission power in comparison with p^+/n-Si:Er diode structures. The experimental results are compared with the model predictions for these structures. The factors limiting the electroluminescence intensity and impact excitation efficiency for erbium ions in tunnel transit-time LEDs are discussed.

DOI: 10.1134/S1063782610110217

1. INTRODUCTION

Doping of silicon and other semiconductor materials with rare earth ions is promising for optoelectronic applications, because optically active media, characterized by a narrow and temperature-independent spectral line, can be formed in this way. These unique properties of materials doped with rare earth ions are explained as follows: the optical activity of these ions is caused by the intraatomic (intraion) transitions in their partially filled 4*f* shell, which is shielded by external 5*s* and 5*p* shells from external effects. In addition, erbium-doped silicon is of interest because it can be used as a basis to design light-emitting devices compatible with the silicon technology and emitting in one of the transparency windows of optical fibers: $^4I_{13/2} \rightarrow {}^4I_{15/2}$ transition in the 4*f* shell of Er^{3+} ion at the wavelength $\lambda \approx 1.54$ μm (see reviews [1–3]).

Investigations showed that impact excitation of Er^{3+} ions is preferred for obtaining high electroluminescence (EL) intensity of Er^{3+} ions at room temperature. This excitation mechanism is implemented in diode structures of the p^+/n-Si:Er type, which emit under reverse bias on the p/n junction in the breakdown regime [4, 5]. The application of impact excitation allows one to significantly suppress the nonradiative relaxation of excited Er^{3+} ions and thus considerably reduce the temperature quenching of erbium luminescence.

The main drawback of p^+/n-Si:Er diode structures is the small width of space-charge region (SCR) in the breakdown mode of p–n junction, which determines the sizes of emitting region and, therefore, the EL intensity under impact excitation of Er^{3+} ions. An increase in the SCR width, which is obtained in p^+/n-Si:Er structures by reducing the doping level of the n-Si:Er layer, causes transformation of the tunnel mechanism of p–n junction breakdown to avalanche and, as a result, sharply decreases the EL intensity of Er^{3+} ions [6, 7]. The factors that reduce the EL intensity of Er^{3+} ions in diodes with avalanche breakdown of p–n junction include impact relaxation of erbium ions by hot electrons [8], nonuniform distribution of the pumping current over the p–n junction area [6], and weak electric field in the SCR of the diode structure [7].

It was shown previously that the limitations related to the development of avalanche breakdown at the SCR extension in p^+/n-Si:Er diode structures can be overcome using diode structures with a special doping profile—in particular, tunnel transit-time $p^+/n^+/n$-Si:Er diodes [9, 10]. Good prospects of $p^+/n^+/n$-Si:Er light-emitting diodes (LEDs) were confirmed by numerical simulation [11] and the first observations of the EL from Er^{3+} ions in $p^+/n^+/n$-Si diode structures [12, 13].

The results of the first studies on tunneling transit-time LEDs justified our concepts about the operation of tunnel transit-time structures and revealed a strong dependence of the electrical and luminescence properties of tunnel transit-time structures on the thickness d of the thin, heavily doped n^+-Si layer [13]. At the same time, many later experiments on tunnel transit-time LEDs, aimed at establishing the factors that limit the erbium EL intensity and quantum efficiency of these devices did not reveal the sharp bell-shaped dependence of the erbium EL intensity on the thickness of the n^+-Si layer, which was reported in [13]. In this paper we generalized the results of these experiments and discussed the factors limiting the EL intensity and efficiency of impact excitation of Er ions in tunnel transit-time LEDs. The experimental results are compared with the model predictions.

2. SIMULATION OF TUNNEL TRANSIT-TIME LED OPERATION

Studies of erbium luminescence in diode structures with different doping profiles and, correspondingly, different electric field distributions over the SCR width for a planar diode structure made it possible to formulate the concepts of optimal field distribution over the SCR width, which would make it possible to maximally increase the erbium EL intensity upon impact excitation of erbium ions. It was shown that the field distribution over the SCR width must be significantly nonuniform: there must be a narrow region of high field near the metallurgical boundary of the *p–n* junction and a fairly wide low-field region. The narrow p^+/n^+ junction (high field region) works in the mode of tunnel breakdown and plays a role of electron injector. The low-field region in the *n*-Si:Er layer serves to heat electrons to the energy E that is necessary to excite erbium ions to the $^4I_{13/2}$ state ($E \approx 0.8$ eV); compensate for the energy loss caused by electron scattering from structural defects and thermal lattice vibrations; and, finally, implement impact excitation of erbium ions [9, 10].

Figure 1 shows the calculated electric field distribution over the SCR width for a tunnel transit-time LED at different thicknesses d of the heavily doped n^+-Si layer. The maximum field in the plane of the $p^+–n^+$ junction, corresponding to the development of tunnel breakdown of this junction, was assumed to be 1400 kV/cm. At a relatively large thickness of the n^+-Si layer (more than 50 nm at the doping level $N_D \approx 2 \times 10^{18}$ cm^{-3}) the field fails to penetrate the *n*-Si:Er layer. In this case, the erbium excitation is minimum and the erbium EL intensity is close to zero. In diodes with a thinner n^+-Si layer an increase in the reverse bias causes field penetration into the *n*-Si:Er layer before the p^+/n^+ junction undergoes tunnel breakdown. With a decrease in the thickness d, the field in the *n*-Si:Er layer increases in the breakdown regime. Correspondingly, the mean energy of the electrons transported through the *n*-Si:Er layer and the probability of impact excitation of erbium ions by the flux of hot electrons increase and the erbium luminescence intensity increases eventually. At the same time, the excess amplification of the electric field in the *n*-Si:Er layer should lead to the development of avalanche breakdown of the *n*-Si:Er layer and, correspondingly, reduce the erbium luminescence intensity. Thus, a decrease in the thickness d of the n^+-Si layer should initiate the transformation of tunneling breakdown of the p^+/n^+ junction into avalanche breakdown of the *n*-Si:Er layer and achievement (at some intermediate d value) of maximum erbium luminescence intensity in the mixed breakdown mode.

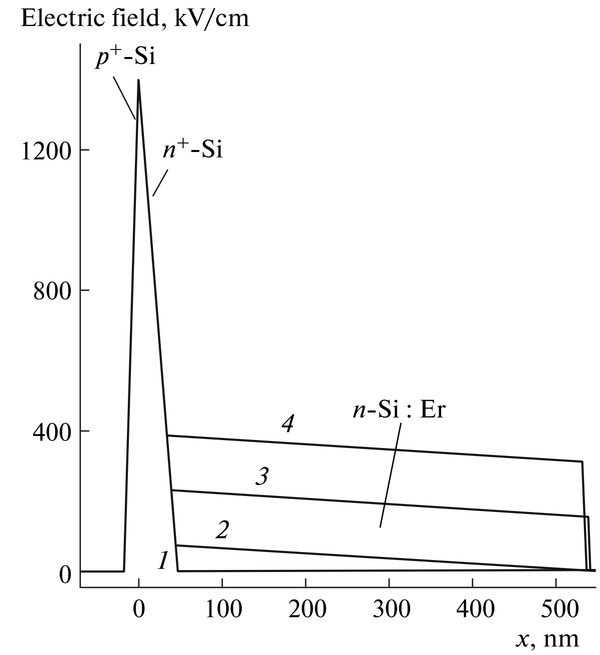

Fig. 1. Electric field distribution over the SCR width in a reverse-biased tunnel transit-time LED. The beginning of the abscissa axis corresponds to the plane of the $p^+–n^+$ junction. The concentrations of free charge carriers in the p^+-Si, n^+-Si, and *n*-Si:Er layers are 5×10^{18}, 2×10^{18}, and 0.01×10^{18} cm^{-3}, respectively. The n^+-Si layer thicknesses are (*1*) 50, (*2*) 40, (*3*) 35, and (*4*) 30 nm.

3. EXPERIMENTAL

The $p^+/n^+/n$-Si:Er structures were grown by sublimation molecular-beam epitaxy (SMBE) [14] on *p*-Si:B (100) substrates with a resistivity of 10–12 Ω cm. The layer parameters were as follows: $d \sim 0.2$ μm and $p \approx 10^{19}$ cm^{-3} (p^+-Si); $d \approx 10–60$ nm and $n \approx 2 \times 10^{18}$ cm^{-3} (n^+-Si); and $d \approx 0.5$ μm, $n \approx 10^{16}$ cm^{-3}, and $N_{Er} \approx 3 \times 10^{18}$ cm^{-3} (*n*-Si:Er). This structure was coated from above by a subcontact layer n^+-Si ($d \approx 0.4$ μm, $n \approx 10^{20}$ cm^{-3}). LEDs for EL measurements were fabricated using the conventional mesa technology, with a mesa area of ~2.2 mm^2. A grid metal contact was deposited on the mesa surface, with 80% of the mesa area left free for radiation exit.

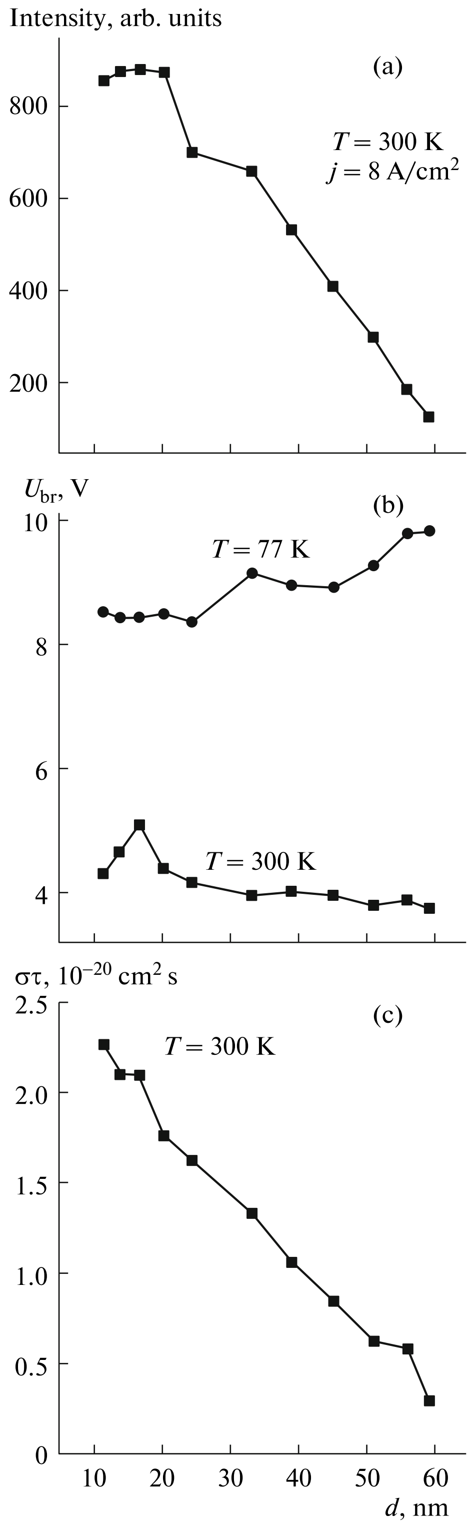

Fig. 2. Dependences of the (a) erbium EL intensity, (b) the breakdown voltages at room and liquid nitrogen temperatures, and (c) the excitation efficiency $\sigma\tau$ for a tunneling transit-time LED on the thickness d of the n^+-Si layer.

EL spectra were excited by pulsed current pumping (pulse width ~4 ms, repetition frequency ~40 Hz, amplitude up to 500 mA) and recorded in the range of 1.0–1.6 μm using a grating monochromator, InGaAs IR photodetector, and a technique of synchronous signal collection.

Current–voltage (I–V) characteristics of the diodes were measured in the pulsed mode. The breakdown voltage U_{br} was determined by extrapolating the straight-line portion of the reverse I–V characteristic to the intersection with the voltage axis. A comparison of the breakdown voltages measured at room (U_{br}^{300}) and liquid nitrogen (U_{br}^{77}) temperatures made it possible to estimate the proximity of the breakdown mechanism to tunnel ($U_{br}^{300}/U_{br}^{77} < 1$), avalanche ($U_{br}^{300}/U_{br}^{77} > 1$), or mixed ($U_{br}^{300}/U_{br}^{77} \approx 1$) modes [15].

4. RESULTS AND DISCUSSION

Figure 2 shows the results of measuring the erbium EL intensity, breakdown voltages U_{br} at room and liquid nitrogen temperatures, and excitation efficiency of Er^{3+} ions as functions of the thickness d of the n^+-Si layer. The excitation efficiency is considered to be the product $\sigma\tau$ of the excitation cross section σ by the lifetime τ of excited Er^{3+}. The excitation efficiency is generally determined by measuring the dependence of the erbium EL intensity I on the pumping current density j (see, for example, [16]):

$$I = I_{max}\frac{\sigma\tau j/q}{1 + \sigma\tau j/q}, \quad (1)$$

where q is the elementary charge.

The dependences obtained are typical of most tunnel transit-time structures that have been studied. At the same time, they differ both from the predictions of the above-considered simplified model of tunneling transit-time LED and from the results of studying the tunnel transit-time LEDs [13].

First, a decrease in the thickness d of the n^+-Si layer is not accompanied by a radical change in the breakdown nature: the breakdown voltages U_{br}^{300} and U_{br}^{77} in the range of thicknesses d = 10–60 nm change only slightly, and the breakdown remains tunneling ($U_{br}^{300} < U_{br}^{77}$). With a decrease in the thickness d of the n^+-Si layer, the difference between U_{br}^{300} and U_{br}^{77} decreases, which is indicative of transformation of the breakdown mechanism into avalanche; however, this transformation is rather slow.

Then, according to the above representations, a decrease in the thickness d of the n^+-Si layer is accompanied by an increase in the erbium EL intensity; we attribute this increase to the electric field amplification in the n-Si:Er emission layer [13]. At the same time, the expected bell-shaped dependence of the

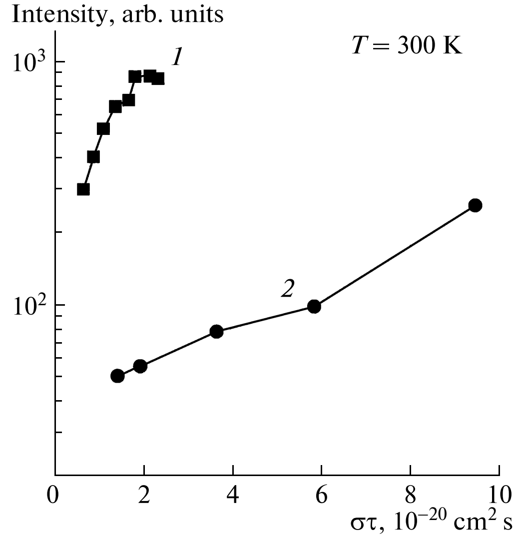

Fig. 3. Relation between the excitation efficiency στ and erbium EL intensity for (*1*) the tunneling transit-time LED and (*2*) p^+/n-Si:Er LED. The EL intensity was measured at a pumping current of 200 mA.

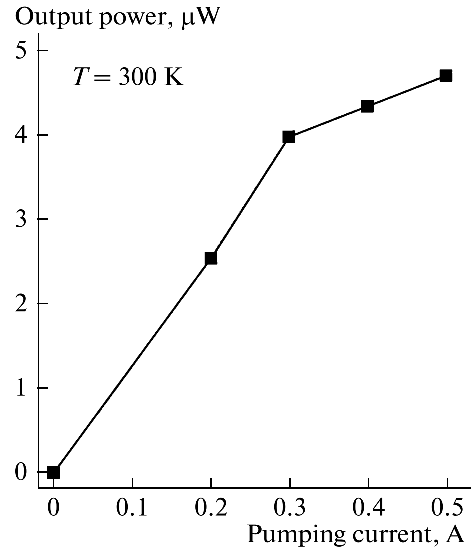

Fig. 4. Dependence of the output power of a tunnel transit-time LED on the pumping current.

EL intensity on the n^+-Si layer thickness, which is generally related to the transformation of LED breakdown mechanism, is absent. In our experiments a decrease in *d* led only to an increase in the EL intensity to a constant value (presence of a plateau). Note that the results in Fig. 2a (absence of bell-shaped dependence) and Fig. 2b (conservation of tunneling breakdown) are quite consistent.

The efficiency of impact excitation of erbium ions in the samples studied increases with a decrease in the n^+-Si layer thickness (Fig. 2c); we also relate this fact to the electric field amplification in the *n*-Si:Er layer. At the same time, the excitation efficiency remains fairly low in comparison with the data on p^+/n-Si:Er LEDs with a constant doping level of the diode base (*n*-Si:Er layer) and triangular electric field profile over the SCR width ($\sigma\tau \approx 10^{-19}$ cm^2 s [6]). The measured erbium EL intensity and excitation efficiency of Er^{3+} ions in a series of tunneling transit-time LEDs (results of this study) and a series of p^+/n-Si:Er LEDs [6] are compared in Fig. 3. In tunneling transit-time LEDs the excitation efficiency was changed by changing the thickness *d* of the n^+-Si layer, while in p^+/n-Si:Er diodes this was done by changing the doping level in the *n*-Si:Er layer.

In p^+/n-Si:Er LEDs the range of variation in στ reaches, as was indicated above, an order of magnitude and, what is more important, the excitation efficiency reaches the value $\sigma\tau \approx 10^{-19}$ cm^2 s (LEDs with a mixed breakdown mechanism), which is unprecedentedly high for p^+/n-Si:Er structures [6, 17]. It can be seen that the excitation efficiency of tunneling transit-time structures is below that of p^+/n-Si:Er structures. Note that the excitation efficiency obtained in tunnel transit-time LEDs corresponds to the characteristic values for p^+/n-Si:Er LEDs emitting in the tunnel breakdown mode, which is also consistent with the results presented in Figs. 2a and 2b.

Nevertheless, provided that the excitation efficiency is the same, the EL intensity of a tunneling transit-time LED is much higher than that of p^+/n-Si:Er diode structures. The difference in the erbium EL intensities for tunneling transit-time and conventional LEDs, which is observed in Fig. 3, is due (approximately equally) to the following two factors: (i) difference in the SCR width in these diode structures ($W \sim 50$–100 nm in the p^+/n-Si:Er structure and $W \sim 500$ nm in the tunnel transit-time structure) and (ii) the difference in the form of the upper metal contact. The point is that p^+/n-Si:Er LEDs were fabricated using a ring metal contact, while the tunnel transit-time LEDs, as was noted above, had a grid contact. Experiments showed that a grid contact is preferred both for improving radiation extraction and for increasing the LED pump efficiency. According to our data, the difference in the erbium EL intensity that is caused by the difference in the SCR width in diode structures, is in the range of three to five for different LEDs, which approximately corresponds to the range of SCR width variation.

The dependence of the total (i.e., emitted into a sphere) power from a tunneling transit-time structure at a wavelength of ~1.5 μm on the pumping current is shown in Fig. 4. The radiation was collected into a solid angle of ~0.3 sr and focused onto the entrance window of a highly sensitive OPHIR-3A IR photodetector. The total power was estimated on the assumption of isotropic directional pattern of the structure. At room temperature the total power was ~ 4.7 μW at a pumping current of ~0.5 A ($j \approx 20$ A/cm^2) and the external quantum efficiency was ~1.5×10^{-5} at a pumping current up to 0.2 A ($j \approx 8$ A/cm^2).

The consideration of the results shown in Figs. 2–4 leads to the following main conclusions. First, we could extend the SCR in a LED structure (approximately to 0.5 μm) without going beyond the tunnel breakdown mode; thus, we confirmed the validity of the main model concepts about the tunneling transit-time LED operation. According to the data in the available publications, the radiation power obtained in the tunneling transit-time LED is the highest for erbium-doped silicon diode structures emitting at room temperature.

Second, the impact excitation efficiency of erbium ions in tunnel transit-time LEDs is below that for p^+/n-Si: Er LEDs. Apparently, the low excitation efficiency of erbium ions in tunnel transit-time LED is caused by the impossibility (at least for most LEDs) of amplifying the electric field in the n-Si:Er layer to the value corresponding to the mixed mechanism of LED breakdown (~300 kV/cm), at which the tunnel and avalanche components would equally contribute to the breakdown current. This suggestion is confirmed by the results of experimental study of the effect of thickness d of the n^+-Si layer on the erbium EL intensity and the mechanism of breakdown of tunneling transit-time LEDs (Figs. 2a, 2b).

According to the generally accepted concepts, the increase in the impact excitation efficiency of Er^{3+} ions, which is observed in p^+/n-Si:Er LEDs at SCR extension and, correspondingly, enhancement of the avalanche component in the LED breakdown current (see Fig. 3 and data of [6]), are due to the heating of the electrons transported through the diode structure in the breakdown mode; this pattern is confirmed by the increase in $U_{\rm br}$ [6, 17]. In tunneling transit-time LEDs the heating of the electrons transported through the n-Si:Er layer, as well as the increase in the breakdown voltage $U_{\rm br}$, should be caused by a decrease in the thickness of the n^+-Si layer and the corresponding increase in the electric field strength in the n-Si:Er layer (Fig. 1). In our opinion, the impossibility of increasing the electric field in the n-Si:Er layer to a value sufficient for electron heating and transforming the tunnel breakdown into a mixed one by decreasing the n^+-Si layer thickness may be related to the nonuniform distribution of ionized donors and acceptors in the SCR in most investigated diode structures. The results of preliminary calculations suggest that at a small thickness of n^+-Si layer fluctuations in the distribution of ionized donor and acceptor charges in the SCR hinder the development of avalanche breakdown. This hypothesis not only accounts for the experimental results obtained here, but also suggests that their difference from the previous data [13] is due to the difference in the intensity of charge density fluctuations in the LED SCR. Studies aimed at confirming the above-mentioned hypothesis are under way.

5. CONCLUSIONS

We fabricated and investigated tunneling transit-time $p^+/n^+/n$-Si:Er LEDs with an extended SCR and enhanced radiation power at room temperature. In comparison with the previously investigated simpler diode structures of the p^+/n-Si:Er type, the tunneling transit-time LEDs are characterized by a higher (by a factor of 3–5) emission power but have a lower excitation efficiency. The factors determining the low excitation efficiency of erbium ions in tunneling transit-time LEDs may be related to both technology and the features of electric breakdown development in nanoscale-doped diode structures.

ACKNOWLEDGMENTS

This study was supported by the Russian Foundation for Basic Research (project no. 09-02-00898), programs of the Russian Academy of Sciences, and the Federal Target Program (state contract no. 02.740.11.0117).

REFERENCES

1. A. Polman, J. Appl. Phys. **81**, 1 (1997).
2. A. J. Kenyon, Semicond. Sci. Technol. **20**, R65 (2005).
3. N. Q. Vinh, N. N. Ha, and T. Gregorkiewicz, Proc. IEEE **97**, 1269 (2009).
4. G. Franzo, F. Priolo, S. Coffa, A. Polman, and A. Carnera, Appl. Phys. Lett. **64**, 2235 (1994).
5. J. Stimmer, A. Reittinger, J. F. Nutzel, H. Holzbrecher, Ch. Buchal, and G. Abstreiter, Appl. Phys. Lett. **68**, 3290 (1996).
6. V. B. Shmagin, D. Yu. Remizov, Z. F. Krasilnik, V. P. Kuznetsov, V. N. Shabanov, L. V. Krasilnikova, D. I. Kryzhkov, and M. N. Drzdov, Fiz. Tverd. Tela **46**, 110 (2004) [Phys. Solid State **46**, 109 (2004)].
7. V. P. Kuznetsov, Yu. Yu. Remizov, V. N. Shabanov, R. A. Rubtsova, M. V. Stepikhova, D. I. Kryzhkov, A. N. Shushunov, O. V. Belova, Z. F. Krasilnik, and G. A. Maksimov, Fiz. Tekh. Poluprovodn. **40**, 868 (2006) [Semiconductors **40**, 846 (2006)].
8. G. V. Hansson, W.-X. Ni, C.-X. Du, A. Elfving, and F. Duteil, Appl. Phys. Lett. **78**, 2104 (2001).
9. V. B. Shmagin, Yu. Yu. Remizov, S. V. Obolensky, D. I. Kryzhkov, M. N. Drozdov, and Z. F. Krasilnik, Fiz. Tverd. Tela **47**, 120 (2005) [Phys. Solid State **47**, 125 (2005)].
10. V. B. Shmagin, S. V. Obolensky, F. Yu. Remizov, V. P. Kuznetsov, and Z. F. Krasilnik, IEEE J. Sel. Top. Quant. Electron. **12**, 1556 (2006).

11. S. V. Obolensky, V. B. Shmagin, V. A. Kozlov, K. E. Kudryavtsev, D. Yu. Remizov, and Z. F. Krasilnik, Semicond. Sci. Technol. **21**, 1459 (2006).

12. D. Yu. Remizov, Z. F. Krasilnik, V. P. Kuzentsov, S. V. Obolensky, and V. B. Shmagin, in *Proc. of the 10th Symp. on Nanophysics and Nanoelectronics* (Nizh. Novgorod, Russia, 2006), vol. 2, p. 348.

13. V. P. Kuznetsov, D. Yu. Remizov, V. B. Shmagin, K. E. Kudryavtsev, V. N. Shabanov, S. V. Obolensky, O. V. Belova, M. V. Kuznetsov, A. V. Kornaukhov, B. A. Andreev, and Z. F. Krasilnik, Fiz. Tekh. Poluprovodn. **41**, 1329 (2007) [Semiconductors **41**, 1312 (2007)].

14. V. P. Kuznetsov and R. A. Rubtsova, Fiz. Tekh. Poluprovodn. **34**, 519 (2000) [Semiconductors **34**, 502 (2000)].

15. S. M. Sze, *Physics of Semiconductor Devices* (Wiley, New York, 1969; Mir, Moscow, 1984), pt. 1, ch. 2.

16. G. Franzo, S. Coffa, F. Priolo, and C. Spinella, J. Appl. Phys. **81**, 2784 (1997).

17. N. A. Sobolev, Yu. A. Nikolaev, A. M. Emel'yanov, K. F. Shtel'makh, P. E. Khakuashev, and M. A. Trishenkov, J. Luminesc. **80**, 315 (1999).

Translated by Yu. Sin'kov